

Aluminum Complexes of Fluorinated Dialkoxy-Diimino Salen-like Ligands: Syntheses, Structures, and Use in Ring-Opening Polymerization of Cyclic Esters

Miloud Bouyahyi, Ekaterina Grunova, Nicolas Marquet, Evgueni Kirillov, Christophe M. Thomas, Thierry Roisnel, and Jean-François Carpentier*

Catalysis and Organometallics, UMR 6226 Sciences Chimiques de Rennes, CNRS-University of Rennes 1, 35042 Rennes Cedex, France

Received July 10, 2008

The coordination chemistry of new fluorinated dialkoxy-diimino ligands onto Al(III) centers has been studied. Diimino-diols $(\text{CF}_3)_2\text{C}(\text{OH})\text{CR}^1_2\text{C}(\text{R}^2)=\text{N}-\text{R}^3-\text{N}=\text{C}(\text{R}^2)\text{CR}^1_2\text{C}(\text{OH})(\text{CF}_3)_2$ ($\{\text{ON}^{\text{Et}}\text{NO}\}\text{H}_2$, $\text{R}^1 = \text{H}$, $\text{R}^2 = \text{Me}$, $\text{R}^3 = \text{C}_2\text{H}_4$; $\{\text{ON}^{\text{Cy}}\text{NO}\}\text{H}_2$, $\text{R}^1 = \text{H}$, $\text{R}^2 = \text{Me}$, $\text{R}^3 = \text{trans-1,2-cyclohexyl}$; $\{\text{MeON}^{\text{Et}}\text{NO}\}\text{H}_2$, $\text{R}^1 = \text{Me}$, $\text{R}^2 = i\text{Pr}$, $\text{R}^3 = \text{C}_2\text{H}_4$) react selectively with AlMe_3 , AlMe_2Cl , and $\text{Al}(\text{OiPr})_3$ to give the corresponding complexes $\{\text{ON}^{\text{Et}}\text{NO}\}\text{AlX}$ ($\text{X} = \text{Me}$, **1**; Cl , **2**; OiPr , **3**), $\{\text{ON}^{\text{Cy}}\text{NO}\}\text{AlX}$ ($\text{X} = \text{Me}$, **5**; Cl , **6**; OiPr , **7**), and $\{\text{MeON}^{\text{Et}}\text{NO}\}\text{AlX}$ ($\text{X} = \text{Me}$, **8**; Cl , **9**) with concomitant alkane or alcohol elimination, respectively. Single-crystal X-ray diffraction studies revealed that complexes **2**, **5**, **7**, **8**, and **9** are mononuclear in the solid state with distorted trigonal-bipyramidal to square-pyramidal geometries. Complexes **1–9** were also characterized in CD_2Cl_2 solution by ^1H , ^{13}C , and ^{19}F NMR spectroscopy. Only one symmetric isomer was observed for complexes **1–7**, but mixtures of two isomers (one symmetric, one dissymmetric on the NMR time scale) were observed for complexes **8** and **9**. The Al-OiPr complexes **3** and **7** are effective initiators for the ring-opening polymerization of ϵ -caprolactone and racemic lactide, giving polymers with high molecular weights (M_n up to 37 500 g mol^{-1}) and relatively narrow polydispersities ($M_w/M_n = 1.08\text{--}1.91$). The PLAs produced, both under slurry or melt conditions, with either achiral complex **3** or chiral complex **7**, have a highly isotactic-enriched stereoblock microstructure ($P_{\text{meso}} = 0.87$).

Introduction

Aluminum alkoxide complexes modified by ancillary ligands have attracted much attention in the past decade as catalysts/initiators for the ring-opening polymerization (ROP) of cyclic esters¹ such as ϵ -caprolactone ($\epsilon\text{-CL}$)² and lactide (LA),³ a renewable resource. The resulting polyesters are of high topical interest due to their biodegradability/biocompatibility and the practical applications derived thereof. A major interest of these so-called single-site aluminum catalysts is the high degree of control they exhibit over polymerization, resulting in materials with controlled molecular weight and narrow molecular weight distribution. Also, in some cases, fine control of the polymerization stereochemistry appeared feasible, e.g., formation of isotactic-rich polylactides from racemic lactide.^{3d,e} The nature of the ancillary ligand in the Al coordination sphere is an

obvious key parameter that determines the steric and electronic properties, and in turn the catalytic performances, of these Al complexes. There is therefore a continuous search for such new ancillaries.

We report herein the preparation of new Al complexes supported by original di(β -hydroxy- β -bis(trifluoromethyl))-diimine ligands. These tetradentate fluorinated dialkoxy-diimino ligands are related to salen-type ligands⁴ in the nature of the coordinating heteroatoms and their overall ONNO disposition/structure. The coordination chemistry of *bidentate* fluorinated alkoxy-imino ligands of the type $[\text{RN}=\text{C}(\text{CF}_3)_2\text{O}]^-$ ⁵ has been studied for metal organic chemical vapor deposition (MOCVD)

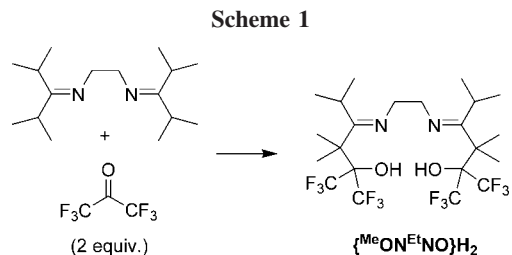
* Corresponding author. Fax: (+33)(0)223-236-939. E-mail: jean-francois.carpentier@univ-rennes1.fr.

(1) For reviews, see: (a) Dechy-Cabaret, O.; Martin-Vaca, B.; Bourissou, D. *Chem. Rev.* **2004**, *104*, 6147. (b) O'Keefe, B. J.; Hillmyer, M. A.; Tolman, W. B. *J. Chem. Soc., Dalton Trans.* **2001**, 2215. (c) Wu, J.; Yu, T.-L.; Chen, C.-T.; Lin, C.-C. *Coord. Chem. Rev.* **2006**, *250*, 602.

(2) (a) Taden, I.; Kang, H.-C.; Massa, W.; Spaniol, T. P.; Okuda, J. *Eur. J. Inorg. Chem.* **2000**, 441. (b) Liu, Y.-C.; Ko, B.-R.; Lin, C.-C. *Macromolecules* **2001**, *34*, 6196. (c) Liao, T.-C.; Huang, Y.-L.; Huang, B.-H.; Lin, C.-C. *Macromol. Chem. Phys.* **2003**, *204*, 885. (d) Alcazar-Roman, L. M.; O'Keefe, B. J.; Hillmyer, M. A.; Tolman, W. B. *J. Chem. Soc., Dalton Trans.* **2003**, 3082. (e) Chen, C.-T.; Huang, C.-A.; Huang, B.-H. *J. Chem. Soc., Dalton Trans.* **2003**, 3799. (f) Chen, C.-T.; Huang, C.-A.; Huang, B.-H. *Macromolecules* **2004**, *37*, 7968. (g) Nomura, N.; Aoyama, T.; Ishii, R.; Kondo, T. *Macromolecules* **2005**, *38*, 5363. (h) Hu, H.; Chen, E. Y.-X. *Organometallics* **2007**, *26*, 5395. (i) Chai, Z.-Y.; Zhang, C.; Wang, Z.-X. *Organometallics* **2008**, *27*, 1626.

(3) (a) Spassky, N.; Wisniewski, M.; Pluta, C.; Le Borgne, A. *Macromol. Chem. Phys.* **1996**, *197*, 2627. (b) Ovitt, T. M.; Coates, G. W. *J. Am. Chem. Soc.* **1999**, *121*, 4072. (c) Ovitt, T. M.; Coates, G. W. *J. Am. Chem. Soc.* **2002**, *124*, 1316. (d) Zhong, Z.; Dijkstra, P. J.; Feijen, J. *Angew. Chem., Int. Ed.* **2002**, *41*, 4510. (e) Nomura, N.; Ishii, R.; Akakura, M.; Aoi, K. *J. Am. Chem. Soc.* **2002**, *124*, 5938. (f) Hornmiron, P.; Marshall, E. L.; Gibson, V. C.; White, A. J. P.; Williams, D. J. *J. Am. Chem. Soc.* **2004**, *126*, 2688. (g) Ma, H.; Melillo, G.; Oliva, L.; Spaniol, T. P.; Englert, U.; Okuda, J. *J. Chem. Soc., Dalton Trans.* **2005**, 721. (h) Lewinski, J.; Horeglad, P.; Wojcik, K.; Justyniak, I. *Organometallics* **2005**, *24*, 4588. (i) Nomura, N.; Ishii, R.; Yamamoto, Y.; Kondo, T. *Chem.-Eur. J.* **2007**, *13*, 4433. (j) Du, H.; Pang, X.; Yu, H.; Zhuang, X.; Chen, X.; Cui, D.; Wang, X.; Jing, X. *Macromolecules* **2007**, *40*, 1904. (k) Chisholm, M. H.; Gallucci, J. C.; Quisenberry, K. T.; Zhou, Z. *Inorg. Chem.* **2008**, *47*, 2613. (4) Atwood, D. A.; Harvey, M. J. *Chem. Rev.* **2001**, *101*, 37.

(5) (a) Such ligands were first prepared in the coordination sphere of metals ions, i.e., Cu^{2+} , Ni^{2+} , Co^{2+} , Ce^{3+} , Ce^{4+} , by the template condensation of primary (di)amines with the fluorinated β -ketol $\text{MeC}(\text{=O})\text{-CH}_2\text{C}(\text{CF}_3)_2\text{OH}$; see: Martin, J. W. L.; Willis, C. J. *Can. J. Chem.* **1977**, *55*, 2459. (b) Konefal, E.; Loeb, S. J.; Stephan, D. W.; Willis, C. J. *Inorg. Chem.* **1984**, *23*, 538, and references therein.



applications in microelectronics with late transition metals (Ru,⁶ Ir,⁷ Pd,⁶ Cu⁸); their chemistry with oxophilic elements (Ga)⁹ remains largely unexplored. We describe in this article the synthesis and structural characterization of fluorinated dialkoxy-diimino Al complexes. Preliminary studies on the catalytic performances of such discrete Al-isopropoxide complexes in the ROP of ϵ -caprolactone and racemic lactide are also reported; it is shown that the PLAs produced under slurry or melt conditions, with either achiral or chiral Al complexes, have a highly isotactic-enriched stereoblock microstructure.

Results and Discussion

Synthesis and Structure of Pro-ligands and Complexes.

Diimino-diol pro-ligands $\{\text{ON}^{\text{Et}}\text{NO}\}_2\text{H}_2$ and $\{\text{ON}^{\text{Cy}}\text{NO}\}_2\text{H}_2$ were prepared by the condensation of the fluorinated aldol $(\text{CF}_3)_2\text{C}(\text{OH})\text{CH}_2\text{C}(\text{O})\text{CH}_3$ with the corresponding primary diamines [1,2-ethylenediamine and *trans*-1,2-cyclohexyldiamine, respectively], in the presence of montmorillonite as a catalyst, as recently described by us.¹⁰ The new “permethylated” diimino-diol pro-ligand $\{\text{MeON}^{\text{Et}}\text{NO}\}_2\text{H}_2$ was prepared via the noncatalyzed reaction of *N,N'*-bis(diisopropylmethylidene)ethylene-1,2-diamine with 2 equiv of anhydrous hexafluoroacetone (Scheme 1).¹¹ This alkylation reaction takes place selectively at the two isopropyl groups *trans* to the ethylene bridge, presumably because the latter groups are less sterically encumbered than those *cis* to the ethylene bridge. The solid-state structures of $\{\text{ON}^{\text{Cy}}\text{NO}\}_2\text{H}_2$ and $\{\text{MeON}^{\text{Et}}\text{NO}\}_2\text{H}_2$ were determined by X-ray diffraction studies, which revealed in both cases the presence of strong intramolecular $=\text{N}\cdots\text{H}-\text{O}$ hydrogen bonding on each half-side of the molecules (Figures 1 and 2, Table 1).

Reactions of the diprotio pro-ligand $\{\text{ON}^{\text{Et}}\text{NO}\}_2\text{H}_2$ with AlMe_3 and AlMe_2Cl proceeded cleanly in THF at 50–60 °C, via methane elimination, to afford the corresponding methyl and chloride complexes $\{\text{ON}^{\text{Et}}\text{NO}\}_2\text{AlX}$ **1** and **2**, which were isolated in 67% and 60% yields, respectively (Scheme 2). The analogous alcohol elimination reaction from $\text{Al}(\text{O}i\text{Pr})_3$ was found to proceed more slowly [as expected from the lower basicity of this Al precursor], and the isopropoxide complex **3** was recovered in 36% yield after heating for 3 days at 80 °C in toluene. In the same way, the methyl, chloride, and isopropoxide complexes **5–7** derived from the *trans*-cyclohexyl-bridged ligand were prepared from $\{\text{ON}^{\text{Cy}}\text{NO}\}_2\text{H}_2$ (either as a racemic mixture and/or enantiomerically pure) and isolated in 63%, 81%,

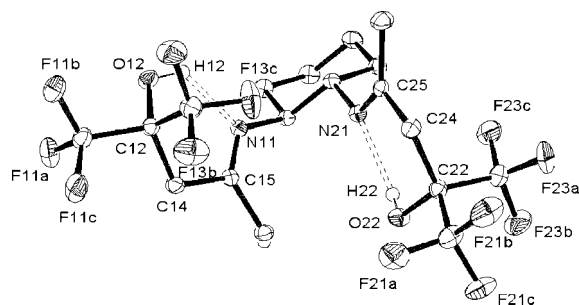


Figure 1. ORTEP view of diimino-diol $\{\text{ON}^{\text{Cy}}\text{NO}\}_2\text{H}_2$ depicted with 50% thermal ellipsoids. Hydrogen atoms bound to C atoms are omitted for clarity. Selected bond lengths (Å) and angles (deg): N(11)–C(12), 1.274(2); N(21)–C(25), 1.273(2); O(12)–C(12), 1.398(2); O(22)–C(22), 1.394(2); O(12)–H(12), 0.840(2); O(22)–H(22), 0.839(2); N(11)–H(12), 2.017(2); N(21)–H(22), 2.000(2); N(11)–C(15)–C(14), 118.1(1); N(21)–C(25)–C(24), 118.0(1).

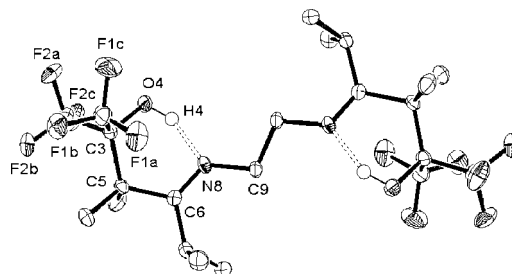


Figure 2. ORTEP view of diimino-diol $\{\text{MeON}^{\text{Et}}\text{NO}\}_2\text{H}_2$ depicted with 70% thermal ellipsoids. Hydrogen atoms bound to C atoms are omitted for clarity. Selected bond lengths (Å) and angles (deg): N(8)–C(6), 1.274(3); O(4)–C(3), 1.401(2); O(4)–H(4), 0.90(3); N(8)–H(4), 1.681(3); N(8)–C(6)–C(5), 118.2(2).

and 56% yields, respectively (Scheme 2). Using the pro-ligand $\{\text{MeON}^{\text{Et}}\text{NO}\}_2\text{H}_2$, the corresponding methyl and chloride aluminum complexes **8** and **9** were prepared in 68% and 62% yield, respectively, but the reaction with $\text{Al}(\text{O}i\text{Pr})_3$ failed to give clean products (Scheme 2).

All compounds were isolated as colorless, air-sensitive powders, which are almost insoluble in aliphatic hydrocarbons (pentane, hexane), moderately soluble in aromatic hydrocarbons (benzene, toluene), and soluble in dichloromethane and THF. Expectedly, complexes **5–7**, which bear a cyclohexyl backbone, and complexes **8** and **9**, which derive from the “permethylated” ligand, are more soluble than their simple ethyl-bridged analogues **1–3**. Single crystals of **5**, **7**, and **8** that proved suitable for X-ray diffraction studies were grown from dichloromethane or toluene solutions.

The solid-state structures of **5**, **7**, **8**, and **9** all feature a monomeric molecule with a five-coordinated aluminum center in a geometry best described as distorted trigonal bipyramidal (tbp) (Figures 3–6, Table 1). The amount of the distortion can be measured using the geometric calculation $\tau = (\beta - \alpha)/60$,¹² which is 0.71, 0.85,¹³ 0.48, and 0.42, respectively. The low τ values for **8** and **9** indicate a more distorted tbp geometry, with a tendency toward a square-pyramidal (sqp) geometry. This suggests a lower flexibility of the “permethylated” $\{\text{MeON}^{\text{Et}}\text{NO}\}_2$

(6) Liu, Y.-H.; Cheng, Y.-C.; Tung, Y.-L.; Chi, Y.; Chen, Y.-L.; Liu, C.-S.; Peng, S.-M.; Lee, G.-H. *J. Mater. Chem.* **2003**, *13*, 135.

(7) Chen, Y.-L.; Hsu, C.-C.; Song, Y.-H.; Chi, Y.; Carty, A. J.; Peng, S.-M.; Lee, G.-H. *Chem. Vap. Deposition* **2006**, *12*, 442.

(8) Lay, E.; Song, Y.-H.; Chiu, Y.-C.; Lin, Y.-M.; Chi, Y.; Carty, A. J.; Peng, S.-M.; Lee, G.-H. *Inorg. Chem.* **2005**, *44*, 7226.

(9) Chi, Y.; Chou, T.-Y.; Wang, Y.-J.; Huang, S.-F.; Carty, A. J.; Scoles, L.; Udachin, K. A.; Peng, S.-M.; Lee, G.-H. *Organometallics* **2004**, *23*, 95.

(10) Marquet, N.; Grunova, E.; Kirillov, E.; Bouyahyi, M.; Thomas, C. M.; Carpentier, J.-F. *Tetrahedron* **2008**, *64*, 75.

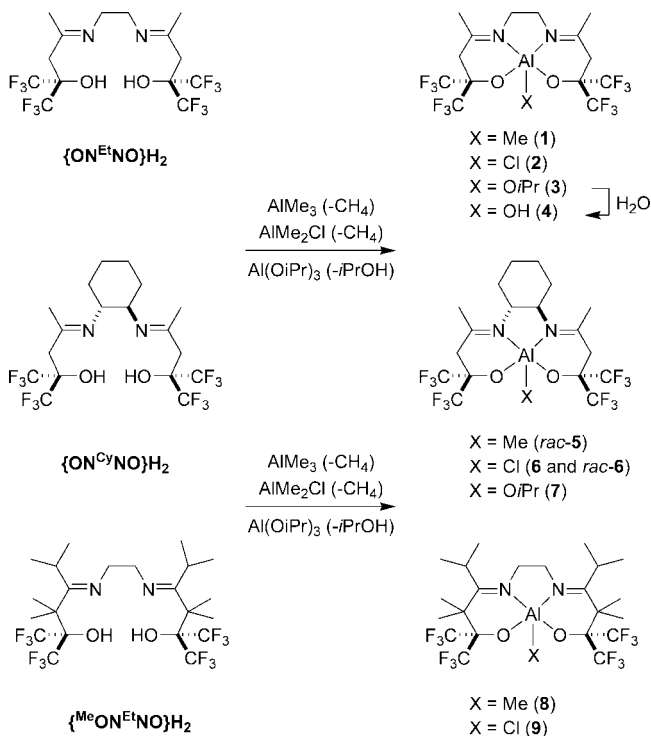
(11) Barten, J. A.; Lork, E.; Rösenthaler, G.-V. *J. Fluor. Chem.* **2004**, *125*, 1039.

(12) The τ value ranges from 0 (perfectly square pyramidal) to 1 (perfectly trigonal bipyramidal). Alpha and beta are the angles that are opposite each other in the *xy* plane (with the Al-X group oriented along the *z*-axis). Addison, A. W.; Rao, T. N.; Reedijk, J.; van Rijn, J.; Verschoor, G. C. *J. Chem. Soc., Dalton Trans.* **1984**, 1349.

(13) Average value for the 4 independent molecules observed in the unit cell of **7**; individual τ values are 0.74, 0.84, 0.89, and 0.95.

Table 1. Summary of Crystal and Refinement Data for Pro-ligands {ON^{Cy}NO}H₂ and {^{Me}ON^{Et}NO}H₂ and Complexes **4, **5**, **7**, **8**, and **9****

	{ON ^{Cy} NO}H ₂	{ ^{Me} ON ^{Et} NO}H ₂	4	5	7	8	9
empirical formula	C ₁₈ H ₂₂ F ₁₂ N ₂ O ₂	C ₂₂ H ₃₂ F ₁₂ N ₂ O ₂	C ₁₄ H ₁₅ AlF ₁₂ N ₂ O ₃	C ₁₉ H ₂₃ AlF ₁₂ N ₂ O ₂	C ₂₁ H ₂₇ AlF ₁₂ N ₂ O ₃	C ₂₃ H ₃₃ AlF ₁₂ N ₂ O ₂	C ₂₂ H ₃₀ AlClF ₁₂ N ₂ O ₂
fw	526.38	584.50	514.26	566.37	610.43	624.49	644.91
cryst syst	triclinic	monoclinic	monoclinic	triclinic	triclinic	orthorhombic	orthorhombic
space group	<i>P</i> $\bar{1}$	<i>P</i> 2 ₁ / <i>n</i>	<i>P</i> 12 ₁ / <i>n</i> 1	<i>P</i> $\bar{1}$	<i>P</i> $\bar{1}$	<i>F</i> 2 _{dd}	<i>F</i> 2 _{dd}
<i>a</i> , Å	12.0774(5)	7.3782(16)	11.0304(7)	8.0836(4)	10.5749(13)	12.3309(8)	12.2935(7)
<i>b</i> , Å	12.4309(5)	22.163(5)	13.3518(9)	10.2938(6)	15.880(2)	26.0824(19)	25.7402(14)
<i>c</i> , Å	16.7774(6)	7.7542(14)	13.8804(10)	15.0534(7)	16.688(2)	33.405(2)	33.4121(19)
α , deg	74.731(2)	90	90	102.211(3)	70.161(7)	90	90
β , deg	89.694(2)	91.228(7)	112.863(3)	105.267(2)	79.861(7)	90	90
γ , deg	66.091(2)	90	90	100.619(2)	85.599(7)	90	90
volume, Å ³	2206.69(15)	1267.7(5)	1883.6(2)	1142.17(10)	2594.5(6)	10743.7(12)	10572.8(10)
Z	4	2	4	2	4	16	16
density, Mg m ⁻³	1.584	1.531	1.813	1.647	1.563	1.544	1.621
abs coeff, mm ⁻¹	0.171	0.157	0.245	0.207	0.191	0.184	0.288
<i>F</i> (000)	1072	604	1032	576	1248	5152	6168
cryst size, mm	0.17 × 0.25 × 0.40	0.06 × 0.15 × 0.38	0.03 × 0.05 × 0.12	0.25 × 0.40 × 0.45	0.03 × 0.10 × 0.30	0.33 × 0.54 × 0.58	0.19 × 0.25 × 0.39
θ range, deg	2.01 to 27.52	2.91 to 27.48	2.02 to 27.50	2.63 to 27.51	2.91 to 27.48	2.93 to 27.45	3.42 to 27.48
limiting indices	-15 ≤ <i>h</i> ≤ 15, -15 ≤ <i>k</i> ≤ 16, -21 ≤ <i>l</i> ≤ 21	-9 ≤ <i>h</i> ≤ 9, -28 ≤ <i>k</i> ≤ 28, -10 ≤ <i>l</i> ≤ 9	-14 ≤ <i>h</i> ≤ 12, -14 ≤ <i>k</i> ≤ 17, -15 ≤ <i>l</i> ≤ 18	-10 ≤ <i>h</i> ≤ 10, -13 ≤ <i>k</i> ≤ 13, -19 ≤ <i>l</i> ≤ 19	-13 ≤ <i>h</i> ≤ 13, -20 ≤ <i>k</i> ≤ 20, -21 ≤ <i>l</i> ≤ 21	-15 ≤ <i>h</i> ≤ 15, -33 ≤ <i>k</i> ≤ 30, -43 ≤ <i>l</i> ≤ 42	-15 ≤ <i>h</i> ≤ 14, -33 ≤ <i>k</i> ≤ 31, -47 ≤ <i>l</i> ≤ 21
reflns collected	34 996	8311	24 665	11 432	30 948	25 931	16 770
reflns unique [<i>I</i> > 2 σ (<i>I</i>)]	10 098 (8507)	2819 (2434)	4318 (3216)	5172 (4572)	11 810 (5140)	6133 (5980)	5531 (4976)
data/restraints/params	10 098/0/613	2819/0/179	4318/0/292	5172/0/331	11 810/1/720	6133/1/445	5531/ 1/369
goodness-of-fit on <i>F</i> ²	1.067	1.189	1.073	1.025	0.933	1.080	1.060
<i>R</i> ₁ [<i>I</i> > 2 σ (<i>I</i>) (all data)]	0.0398 (0.0484)	0.0603 (0.0727)	0.0369 (0.0591)	0.0415 (0.0470)	0.0700 (0.1877)	0.0382 (0.0394)	0.0418 (0.0486)
<i>wR</i> ₂ [<i>I</i> > 2 σ (<i>I</i>) (all data)]	0.1151 (0.1259)	0.1128 (0.1173)	0.0955 (0.1117)	0.1082 (0.1124)	0.1103 (0.1482)	0.0937 (0.0945)	0.0988 (0.1030)
largest diff, e Å ⁻³	0.573 and -0.526	0.341 and -0.242	0.453 and -0.455	0.500 and -0.321	0.387 and -0.356	0.865 and -0.427	0.794 and -0.315

Scheme 2

ligand backbone, as compared to {ON^{Et}NO} and {ON^{Cy}NO}, similar to that found in Al-salen type complexes.⁴ The X ligand [C(31) of Me in **5**; O(47) of *OiPr* in **7**; C(41) of Me in **8**; Cl(1) in **9**] and one N atom [N(7) in **5**; N(23) in **7**; N(32) in **8**; N(31) in **9**] together with the opposite O atom [O(2) in **5**; O(34) in **7**; O(1) in **8** and **9**] of the tetradentate ligand lie in equatorial positions, while the other O atom [O(1) in **5**; O(20) in **7**; O(21)

in **8**; O(31) in **9**] and opposite N atom [N(17) in **5**; N(26) in **7**; N(12) in **8**; N(1) in **9**] of the tetradentate ligand occupy the axial positions. Consistent with the observed *tbp* geometry, the Al–N_{axial} bond distance [Al–N(17), 2.200(1) Å in **5**; Al–N(26), 2.11(1) Å in **7**; Al(1)–N(12), 2.151(2) in **8**; Al(1)–N(1), 2.087(2) Å in **9**] is significantly longer (i.e., ca. 0.1–0.2 Å) than the Al–N_{equa} [Al–N(7), 2.012(1); Al–N(23), 2.01(1); Al–N(32), 2.017(2); Al(1)–N(31), 1.985(2) Å, respectively]. The same trend applies to the Al–O bonds involving the O atoms of the ligands, though it is not as pronounced, with the axial bonds (range: 1.780–1.834 Å) being ca. 0.03–0.07 Å longer than the equatorial ones (range: 1.754–1.778 Å). The Al–O bond distances are longer than those expected for a terminal Al–O alkoxide bond (typically 1.68–1.72 Å),¹⁴ which may result from constraints associated with the Al chelate. The Al–O and Al–N bond distances in **9** are slightly shorter than the corresponding ones in **8**, probably reflecting the lower electron density at the metal center due to the replacement by a Cl atom of the Me group.

Overall, the structural features of **5**, **7**, **8**, and **9** are reminiscent of those observed for the related fluorous diolate-*diimino* complex {CH₂NMeCH₂C(CF₃)₂O}₂Al(*OiPr*).¹⁵ The most noticeable, but still limited, difference between the latter complex and its diolate-*diimino* congener **7** lies in the N–Al–N bite angle (81.6(2)° vs 76.0(4)° [74.2(4)°, 75.4(4)°, 73.7(4)° for the three other independent molecules], respectively). This indicates that substitution of an imino for an amino group did not induce

(14) Giesbrecht, G. R.; Gordon, J. C.; Clark, D. L.; Scott, B. L.; Watkin, J. G.; Young, K. J. *Inorg. Chem.* **2002**, *41*, 6372.

(15) (a) Lavanant, L.; Chou, T.-Y.; Chi, Y.; Lehmann, C. W.; Toupet, L.; Carpentier, J.-F. *Organometallics* **2004**, *23*, 5450. (b) Amgoune, A.; Lavanant, L.; Thomas, C. M.; Chi, Y.; Welter, R.; Dagonne, S.; Carpentier, J.-F. *Organometallics* **2005**, *24*, 6279. (c) Kirillov, E.; Lavanant, L.; Thomas, C. M.; Roisnel, T.; Chi, Y.; Carpentier, J.-F. *Chem.–Eur. J.* **2007**, *13*, 923.

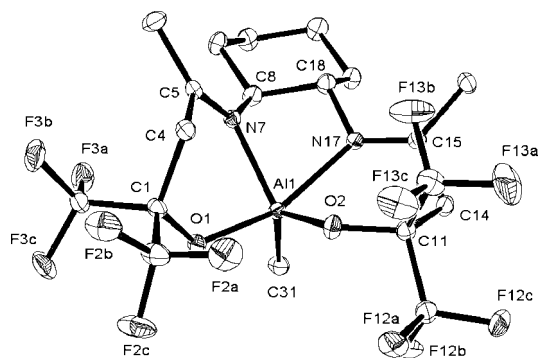


Figure 3. ORTEP view of complex **5** depicted with 50% thermal ellipsoids. Hydrogen atoms are omitted for clarity. Selected bond lengths (Å) and angles (deg): Al(1)–C(31), 1.97(2); Al(1)–O(1), 1.834(1); Al(1)–O(2), 1.767(1); Al(1)–N(7), 2.012(1); Al(1)–N(17), 2.200(1); O(2)–Al(1)–O(1), 94.45(5); O(2)–Al(1)–C(31), 123.30(7); O(1)–Al(1)–C(31), 100.78(6); O(2)–Al(1)–N(7), 117.50(6); O(1)–Al(1)–N(7), 88.47(5); C(31)–Al(1)–N(7), 117.20(7); O(2)–Al(1)–N(17), 86.63(5); O(1)–Al(1)–N(17), 159.99(5); C(31)–Al(1)–N(17), 95.22(6); N(7)–Al(1)–N(17), 73.46(5); N(7)–C(5), 1.280(2); N(17)–C(15), 1.280(2); N(7)–C(5)–C(4), 115.41(14); N(17)–C(15)–C(14), 116.00(14).

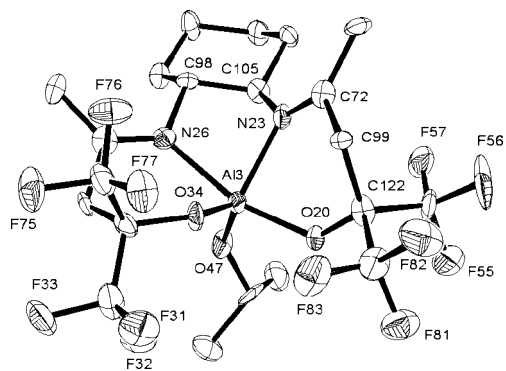


Figure 4. ORTEP view of complex **7** depicted with 50% thermal ellipsoids. Hydrogen atoms are omitted for clarity. Selected bond lengths (Å) and angles (deg) [data in brackets refer to the other three independent molecules]: O(47)–Al(3), 1.717(9) [1.703(8), 1.707(8), 1.725(9)]; O(20)–Al(3), 1.806(8) [1.813(8), 1.805(9), 1.817(9)]; O(34)–Al(3), 1.777(8) [1.773(8), 1.769(8), 1.744(8)]; N(23)–Al(3), 2.01(1) [2.03(1), 2.02(1), 1.99(1)]; N(26)–Al(3), 2.11(1) [2.12(1), 2.07(1), 2.23(1)]; O(34)–Al(3)–O(20), 96.7(4) [96.0(4), 98.0(4), 96.1(4)]; O(47)–Al(3)–O(34), 124.2(5) [125.1(4), 123.2(4), 123.5(4)]; O(47)–Al(3)–O(20), 100.1(4) [96.0(4), 100.5(4), 97.7(4)]; N(23)–Al(3)–N(26), 76.0(4) [74.2(4), 75.4(4), 73.7(4)]; O(34)–Al(3)–N(26), 88.6(4) [89.5(4), 89.4(4), 87.5(4)].

significant constraint within the six-membered N–Al–O metallacycles.

The most worthy and meaningful structural comparison for these new diimino-diolate complexes is undoubtedly with Al-salen (i.e., diimino-bisphenolate) complexes,⁴ since both incorporate similar ligand frameworks. Metrical data, i.e., Al–O, Al–N, Al–X bond distances and the corresponding bond angles, compare well within those two classes of complexes. However, while Al-salen complexes usually adopt a [distorted] sqb geometry, that is, “in-plane” coordination of the diimino-bis(phenolate) ligand,⁴ complexes **5**, **7**, **8**, and **9** have a [distorted] tpb geometry (*vide supra*). Obviously, this change is related to the replacement of rigid phenolate rings in salen ligands by sp³-hybridized alkoxide groups in the ligands of the present study, which results in larger flexibility.

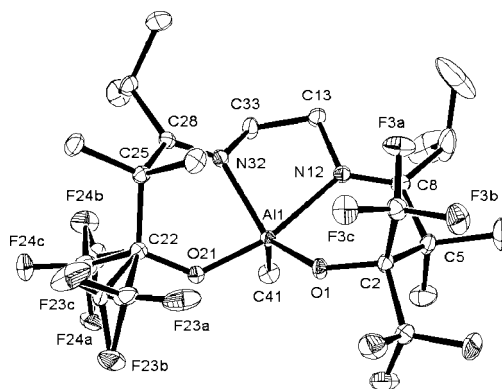


Figure 5. ORTEP view of complex **8** depicted with 50% thermal ellipsoids. Hydrogen atoms are omitted for clarity. Selected bond lengths (Å) and angles (deg): Al(1)–C(41), 1.980(2); Al(1)–O(1), 1.778(1); Al(1)–O(21), 1.807(2); Al(1)–N(12), 2.151(2); Al(1)–N(32), 2.017(2); O(21)–Al(1)–O(1), 94.31(7); O(21)–Al(1)–C(41), 101.78(8); O(1)–Al(1)–C(41), 121.69(8); O(21)–Al(1)–N(32), 88.97(7); O(1)–Al(1)–N(12), 84.87(7); C(41)–Al(1)–N(12), 94.20(8); O(21)–Al(1)–N(12), 161.58(7); O(1)–Al(1)–N(32), 132.84(7); C(41)–Al(1)–N(32), 103.40(8); N(12)–Al(1)–N(32), 78.36(6); N(12)–C(8), 1.271(3); N(32)–C(28), 1.279(3); N(12)–C(8)–C(5), 119.61(17); N(32)–C(28)–C(25), 116.38(16).

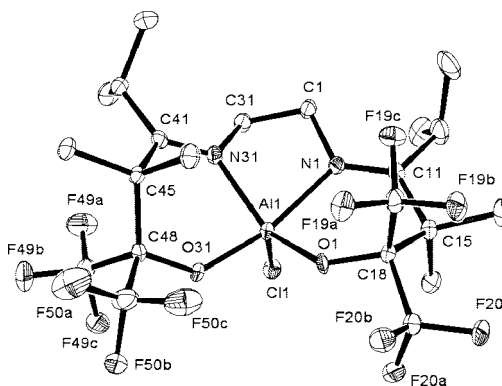


Figure 6. ORTEP view of complex **9** depicted with 50% thermal ellipsoids. Hydrogen atoms are omitted for clarity. Selected bond lengths (Å) and angles (deg): Al(1)–Cl(1), 2.184(1); Al(1)–O(1), 1.754(2); Al(1)–O(31), 1.780(2); Al(1)–N(1), 2.087(2); Al(1)–N(31), 1.985(2); O(31)–Al(1)–O(1), 95.82(9); O(31)–Al(1)–Cl(1), 100.00(7); O(1)–Al(1)–Cl(1), 116.08(8); O(31)–Al(1)–N(31), 89.32(10); O(1)–Al(1)–N(1), 86.87(9); Cl(1)–Al(1)–N(1), 91.62(7); O(31)–Al(1)–N(1), 165.39(10); O(1)–Al(1)–N(31), 140.28(10); Cl(1)–Al(1)–N(31), 101.59(7); N(1)–Al(1)–N(31), 79.62(10); N(1)–C(11), 1.283(4); N(31)–C(41), 1.293(4); N(1)–C(11)–C(15), 120.4(2); N(31)–C(41)–C(45), 116.1(2).

Upon attempting to grow single crystals of isopropoxide complex **3**, adventitious hydrolysis occurred and crystals of the corresponding hydroxo complex **4** were isolated (Scheme 2). An X-ray diffraction study revealed that this compound adopts in the solid state a dimeric structure with μ -bridging hydroxy groups (Figure 7, Table 1). The Al centers are thus in a slightly distorted octahedral environment; in particular, the central Al₂O₂ ring is perfectly planar. This octahedral environment forces also the {^{Me}ON^{Et}NO} ligand to adopt a non-“in-plane” coordination, with the O and N atoms each occupying both an equatorial and an axial site. Despite this difference in the coordination geometry, the bond distances and angles within the Al–{^{Me}ON^{Et}NO} moiety in **4** are quite similar to those in **8**. The Al–O bridge distances and O–Al–O bond angles involving the μ -hydroxy groups are in the known range (Al–O, 1.81–1.89

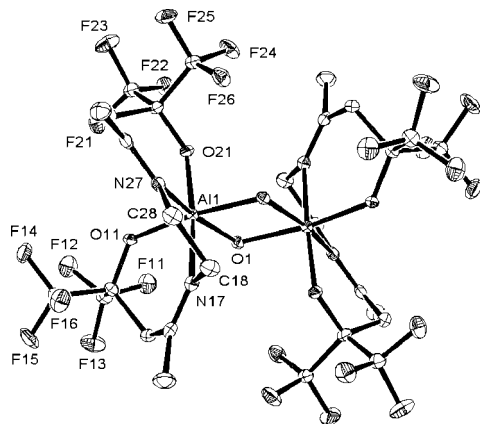


Figure 7. ORTEP view of complex **4** depicted with 50% thermal ellipsoids. All hydrogen atoms are omitted for clarity. Selected bond lengths (Å) and angles (deg): Al(1)–O(21), 1.821(1); Al(1)–O(11), 1.823(1); Al(1)–O(1), 1.848(2); Al(1)–O(1_1), 1.914(2); Al(1)–N(27), 2.061(2); Al(1)–N(17), 2.086(2); O(21)–Al(1)–O(11), 93.93(6); O(21)–Al(1)–O(1), 95.53(7); O(11)–Al(1)–O(1), 99.31(6); O(21)–Al(1)–O(1_1), 92.83(7); O(11)–Al(1)–O(1_1), 172.20(7); O(1)–Al(1)–O(1_1), 76.16(7); O(21)–Al(1)–N(27), 92.13(6); O(11)–Al(1)–N(27), 95.52(6); O(1)–Al(1)–N(27), 162.78(7); O(1_1)–Al(1)–N(27), 88.10(6); O(21)–Al(1)–N(17), 168.04(7); O(11)–Al(1)–N(17), 86.88(7); O(1)–Al(1)–N(17), 96.11(7); O(1_1)–Al(1)–N(17), 87.31(7); N(27)–Al(1)–N(17), 75.92(7).

Å; O–Al–O, 75.0–79.6°) for other dimeric hydroxy-bridged Al complexes with five- or six-coordinated Al centers.¹⁶

Solution NMR Studies of Complexes. NMR experiments were carried out (in CD₂Cl₂) to examine the solution structures of the complexes, and in particular to investigate whether any other geometric isomers could be detected.

The room-temperature ¹H NMR spectra of {ON^{Et}NO}AIX complexes **1–3** all exhibit a single set of sharp resonances consistent with a sole symmetric species present in solution. In particular, one signal is observed for both NC-Me groups, while the hydrogens of the CHHC(CF₃)₂ groups are diastereotopic and appear as an AB system. The uniqueness and high symmetry of these species in CD₂Cl₂ solution at room temperature are corroborated by the observation of a single set of resonances in the ¹³C NMR spectrum, which includes, among others, a single resonance for the NCH₂CH₂N bridge. Also, two sharp quartets of equal intensity are observed in the ¹⁹F{¹H} NMR spectrum (Figure 8), indicating that the two CF₃ groups within each C(CF₃)₂ moiety are nonequivalent. No change in the ¹H NMR spectra of these complexes was noticed in the temperature range 213–313 K (except a slight dependence of some chemical shifts, but these resonances did not broaden). Overall, these data are consistent with the presence of a unique (>98%) species in solution, having either a trigonal-bipyramidal or square-pyramidal structure, as observed in the solid state for complexes **5** and **7**.

The NMR spectra of {ON^{Cy}NO}AIX complexes **5–7** in CD₂Cl₂ solution at room temperature also feature a single set

of sharp resonances, indicative of the presence of a single species. However, these species appear to be dissymmetric on the NMR time scale. Key data include, for instance, two signals for the NC-Me and CH-N=C groups in the ¹H and ¹³C NMR spectra, as well as four sharp quartets of equal intensity in the ¹⁹F{¹H} NMR spectra (Figure 9). These observations are consistent with solution structures for **5–7** identical to those observed in the solid state for complexes **5** and **7** (Figures 3 and 4), considering that the *trans*-1,2-cyclohexyl bridge induces the asymmetry of the molecules. Also, as for complexes **1–3**, no significant change in the ¹H NMR spectra of **5–7** was noticed in the temperature range 213–313 K.

In contrast, the room-temperature ¹H NMR spectra of {^{Me}ON^{Et}NO}AIX complexes **8** and **9** feature broadened resonances, indicative of dynamic phenomena. Upon decreasing the temperature, decoalescence occurs and the 248 K ¹H NMR spectra for both complexes include two sets of sharp resonances for two isomers in a 2:1 and 1.2:1 ratio, respectively. In the case of methyl complex **8**, the major isomer (**8a**) is dissymmetric, as indicated by the four resonances observed for the four magnetically nonequivalent hydrogens of the two CHH-C=N groups (two of these resonances overlapped). On the other hand, the minor isomer (**8b**) is symmetric, as indicated by the only two resonances observed for the latter CHH-C=N groups. A similar situation occurs for chloro complex **9**. In this case, the symmetric species (**9b**), characterized by only two resonances for the CHH-C=N groups, is slightly more abundant than the dissymmetric species (**9a**), which features four distinct resonances for the latter group (see details of the ¹H–¹H COSY NMR spectrum, Figure 10). This (dis)symmetry of **8a/8b** and **9a/9b** was further confirmed by ¹³C NMR spectroscopy (see Experimental Section).

On the basis of these elements, it is reasonable to assume that the symmetric species (**8b**, **9b**) observed in solution have a structure similar to that observed in the solid state for **7** (Figure 4, Scheme 2), that is, sqp geometry, with planar coordination of the diimino-diolate ligand (Chart 1, A). It is also possible that they adopt a tbp geometry with both O atoms in axial positions (D). We speculate that the dissymmetric species (**8b**, **9b**) may adopt either a sqp geometry with one of the two O and two N atoms of the ligands occupying the axial site (B, C), or a tbp geometry with only one O atom in axial position (E). Unfortunately, 2D NMR (NOESY) experiments did not allow discerning within these possibilities.

Preliminary Studies on Ring-Opening Polymerization of ϵ -Caprolactone and *rac*-Lactide. Alkoxide complexes of aluminum are well-established catalysts–initiators for the ring-opening polymerization (ROP) of lactones, such as ϵ -caprolactone (ϵ -CL)² and lactide (LA).³ Catalytic abilities such as activity, productivity, degree of control/livingness, and stereoselectivity in the case of chiral monomers depend crucially on ancillary ligands that define the sterics and electronics around the Al-OR moiety. We were therefore interested in evaluating the abilities of the new fluorinated diolate-diimino platform, considering that (i) {salen}Al-OiPr complexes have been previously shown to have valuable catalytic abilities, especially for controlling the stereoselective ROP of *rac*-lactide,^{3d,e} and (ii) the fluorinated diolate-*diamino* complex {CH₂NMeCH₂C(CF₃)₂O}₂Al(OiPr) has shown high activity toward ϵ -CL.^{15b} Representative results obtained with complexes **3** and **7** in the

(16) (a) Li, X.; Song, H.; Duan, L.; Cui, C.; Roesky, H. W. *Inorg. Chem.* **2006**, *45*, 1912. (b) Zhu, H.; Chai, J.; Jancik, V.; Roesky, H. W.; Merrill, W. A.; Power, P. P. *J. Am. Chem. Soc.* **2005**, *127*, 10170. (c) Zhu, H.; Chai, J.; He, C.; Bai, G.; Roesky, H. W.; Jancik, V.; Schmidt, H.-G.; Noltemeyer, M. *Organometallics* **2005**, *24*, 380. (d) Valle, G. C.; Bombi, G. G.; Corain, B.; Favarato, M.; Zatta, P. *J. Chem. Soc., Dalton Trans.* **1989**, 1513. (e) Nixon, T. D.; Dalgarno, S.; Ward, C. V.; Jiang, M.; Halcrow, M. A.; Kilner, C.; Thornton-Pett, M.; Kee, T. P. *C. R. Chim.* **2004**, *7*, 809. (f) Wei, P.; Atwood, D. A. *Polyhedron* **1999**, *18*, 641. (g) Hoveyda, H. R.; Rettig, S. J.; Orvig, C. *Inorg. Chem.* **1993**, *32*, 4909.

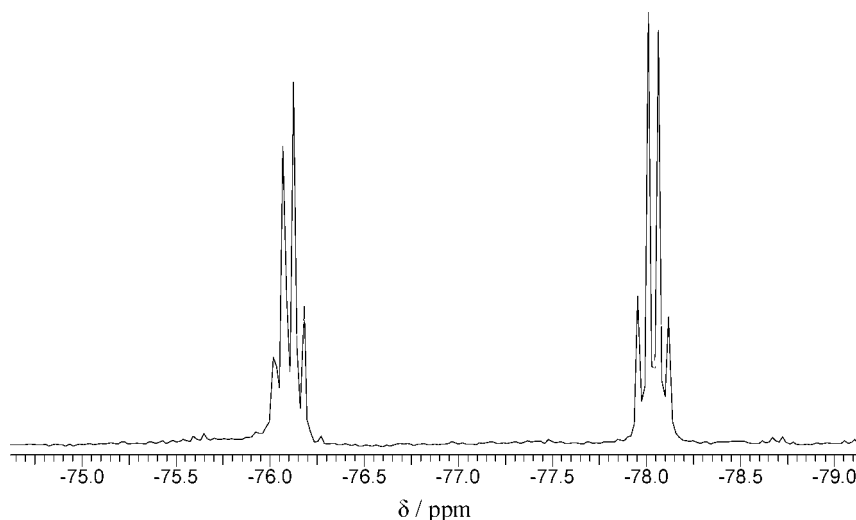


Figure 8. $^{19}\text{F}\{^1\text{H}\}$ NMR spectrum (182 MHz, CD_2Cl_2 , 298 K) of complex $\{\text{ON}^{\text{Et}}\text{NO}\}\text{AlMe}$ (**3**).

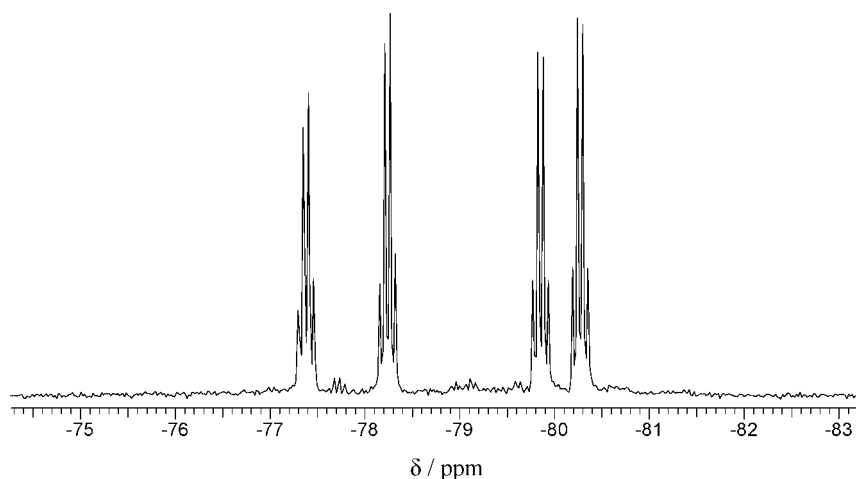


Figure 9. $^{19}\text{F}\{^1\text{H}\}$ NMR spectrum (182 MHz, CD_2Cl_2 , 298 K) of complex $\{\text{ON}^{\text{Cy}}\text{NO}\}\text{Al}(\text{O}i\text{Pr})$ (**7**).

ROP of ϵ -CL and *rac*-LA are summarized in Tables 2 and 3, respectively.

The Al-*OiPr* complexes **3** and **7** are effective initiators for the ROP of ϵ -CL at room temperature (Scheme 3). For solubility reasons (*vide supra*), polymerizations were conducted in either CH_2Cl_2 , THF, or bulk ϵ -CL. Relatively high activities were observed in the latter conditions (THF, bulk), with turnover frequencies (TOF) up to 180–200 h^{-1} for **3** and **7** (entries 3, 7, 10–11). Lower activities in the range 15–75 h^{-1} were observed when lower loadings of **3** or **7** were used ($[\epsilon\text{-CL}]/[\text{Al}] \geq 600$) (entries 5–6 and 12–13); this observation possibly reflects partial deactivation of the catalysts under these conditions. Though comparison with literature data is always hazardous due to possible differences in reaction conditions (temperature, monomer-to-initiator ratio, monomer concentration, solvent and monomer purity,...), these activity data compare favorably with related bis(phenolate) salen and salan aluminum initiator complexes, which are commonly reported to be active from 50 $^\circ\text{C}$,^{2b,c,e,f} and/or afford TOFs 1 order of magnitude lower than **3/7** at room temperature.^{2a,d} A similarly active (TOF up to 300 h^{-1} , $[\epsilon\text{-CL}]/[\text{Al}] < 300$, 25 $^\circ\text{C}$) {salen}AlX-benzyl alcohol system has been recently reported.^{2g} The polymerization rates

of both **3** and **7** are significantly lower in CH_2Cl_2 (TOF = 4–7 h^{-1}) (entries 1–2 and 8). This observation contrasts with the high activity (TOF up to 250 h^{-1}) and productivity (TON up to 1000) observed for $\{\text{CH}_2\text{NMeCH}_2\text{C}(\text{CF}_3)_2\text{O}\}_2\text{Al}(\text{O}i\text{Pr})$ in this solvent.^{15b} The reasons for this marked difference in the behavior of those closely related fluorinated diolate-*diimino* and -*diamino* complexes are still unclear.

The molecular weight distributions are all unimodal, ranging from $M_w/M_n = 1.15$ to 1.86, indicative of a single-site behavior. These polydispersity data are, however, larger than those achieved with $\{\text{CH}_2\text{NMeCH}_2\text{C}(\text{CF}_3)_2\text{O}\}_2\text{Al}(\text{O}i\text{Pr})$ in CH_2Cl_2 ($M_w/M_n = 1.10$ –1.24). The experimental molecular weights determined by GPC (and corrected by a Mark–Houwink factor of 0.56, due to the use of PS standards)¹⁷ are in close agreement with the calculated values for a perfectly living polymerization, provided that rather low monomer-to-Al ratios were used ($[\epsilon\text{-CL}]/[\text{Al}] < 600$). The controlled character of such polymerizations was further evidenced by the sequential polymerization of 200 + 200 equiv of ϵ -CL (entry 7), for which excellent match between the experimental and calculated M_n values was observed, together with no broadening of the molecular weight distribution between the two stages. When larger amounts of ϵ -CL were used ($[\epsilon\text{-CL}]/[\text{Al}] \geq 400$ –600; entries 4–6, 12–13), the observed M_n values were significantly lower than the calculated ones. This observation suggests that transfer reactions

(17) (a) Save, M.; Schappacher, M.; Soum, A. *Macromol. Chem. Phys.* **2002**, *203*, 889. (b) Palard, I.; Soum, A.; Guillaume, S. M. *Macromolecules* **2005**, *38*, 6888.

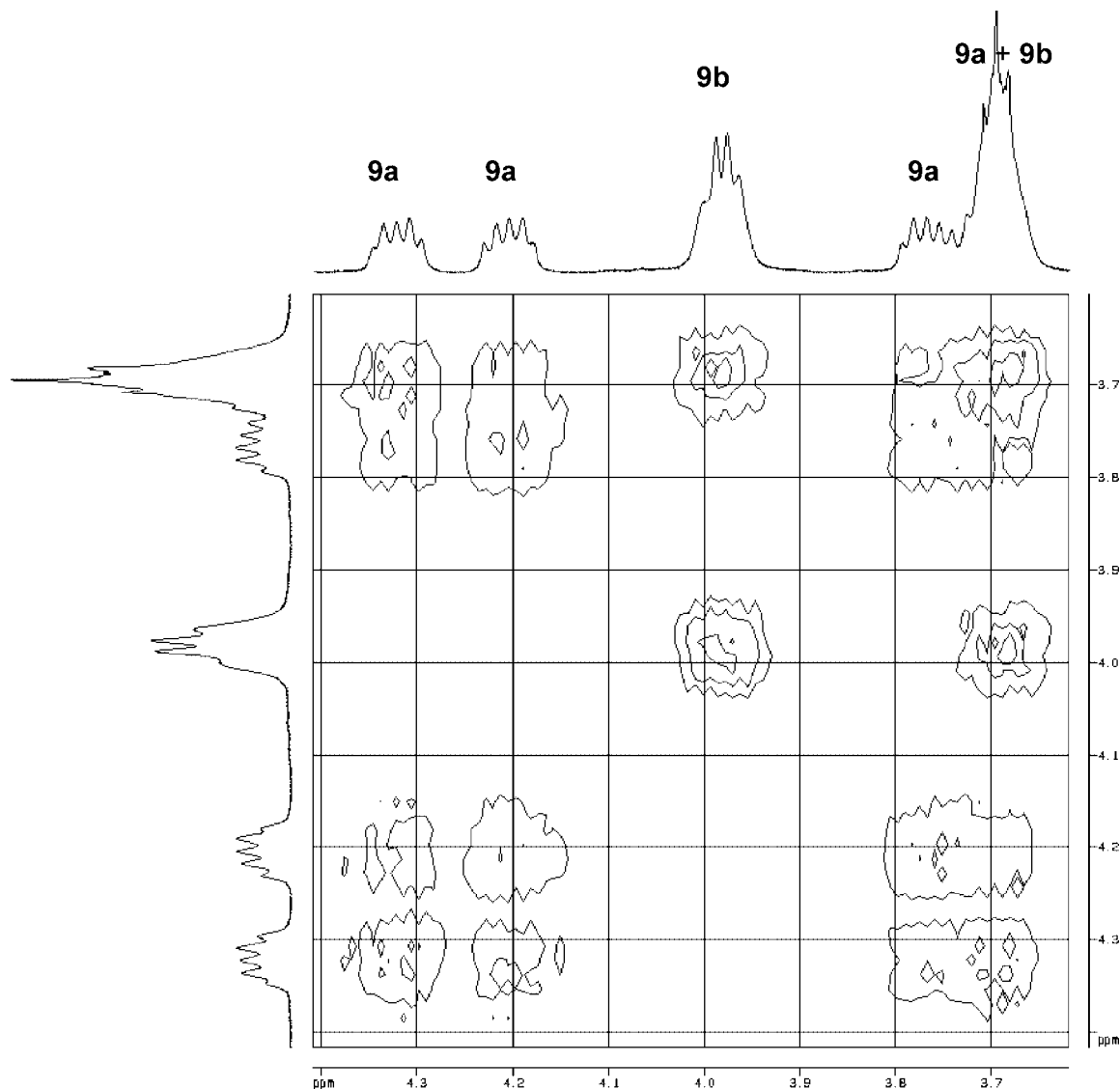
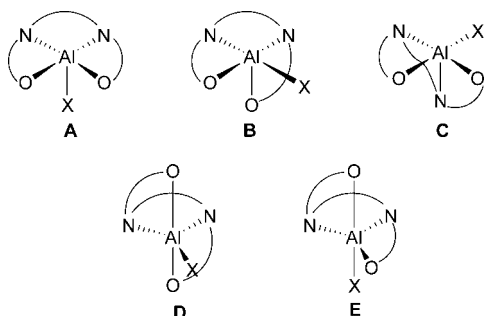


Figure 10. Details of the low-temperature ^1H - ^1H COSY NMR spectrum (500 MHz, CD_2Cl_2 , 248 K) of complex $\{\text{MeON}^{\text{Et}}\text{NO}\}\text{AlCl}$ (**9**), showing individual $\text{CHH}-\text{C}=\text{N}$ resonances for the two isomers **9a/9b**.

Chart 1. Possible Ideal Square-Pyramidal (top) and Trigonal Bipyramidal (bottom) Geometries for Five-Coordinated $\{\text{ONNO}\}\text{AlX}$ Species, with symmetric (A, D) and Dissymmetric (B, C, E) Environments



(to the monomer) take place under such conditions. Evidence for transfer reactions was obtained from ^1H NMR analyses of PCL samples ($M_{n,\text{GPC}} = 16\,500\text{--}18\,200\text{ g mol}^{-1}$), which actually did not feature detectable resonances for an isopropoxy end-group, as might be anticipated in a coordination–insertion mechanism.

The ROP of racemic lactide (*rac*-LA) was also preliminarily investigated with complexes **3** and **7** (Scheme 4, Table 3). Interestingly, a kinetic resolution takes place; that is, these reactions led to the formation of significantly isotactic-enriched stereoblock PLAs, as determined from the methine region of the homodecoupled ^1H NMR spectrum (Figure 11). Up to 81% enrichment for the *mmm* tetrad ($P_{\text{meso}} = 0.87$)¹⁸ was achieved by carrying out the reaction under slurry conditions in toluene at 70 °C with the *chiral* complex **7** (entry 2). It is noteworthy that the *achiral* complex **3** affords almost the same stereoselectivity (entry 1). These P_{meso} values¹⁸ can be compared with those of 0.91 and 0.93, respectively, achieved at 70 °C with Schiff-base Al complexes, namely, achiral $\{1,3\text{-propylene-bridged-Salpen}^{\text{tBu}}\}\text{AlMe}^{\text{3c}}$ and chiral racemic (*trans*-1,2-cyclohexylene-bridged-Salcen^{tBu}) $\text{Al}(\text{O}i\text{Pr})$.^{3d}

The PLAs have relatively narrow polydispersity with M_n values determined by GPC (and corrected by a Mark–Houwink factor of 0.58, due to the use of PS standards)¹⁹ lower than those calculated for a living polymerization (*vide infra*).

(18) The parameter P_{meso} is the probability of forming a new meso-linkage. See: Kasperczyk, J. E. *Macromolecules* **1995**, *28*, 3937.

Table 2. Ring-Opening Polymerization of ϵ -Caprolactone Promoted by $\{\text{ON}^{\text{R}}\text{NO}\}\text{Al}(\text{OiPr})$ Complexes **3 and **7**^a**

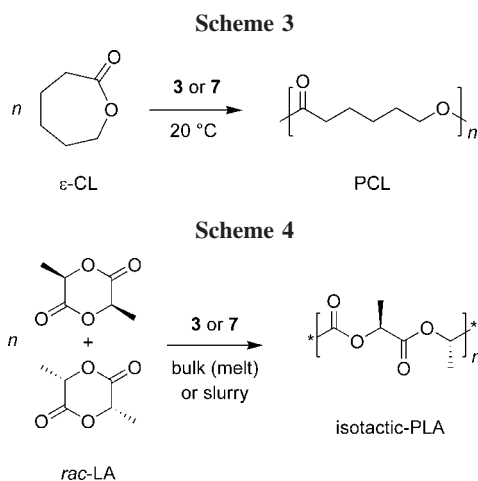
entry	compd	[CL]/[Al]	[CL] (mol/L)	solvent	time ^b (h)	conv ^c (%)	$M_{n,\text{calc}}^d$ (g/mol)	$M_{n,\text{exp}}^e$ (g/mol)	M_w/M_n^e	TOF (h ⁻¹) ^f
1	3	100	2.0	CH ₂ Cl ₂	16	85	9700	11 800	1.18	5
2	3	200	2.0	CH ₂ Cl ₂	24	85	19 400	24 800	1.49	7
3	3	100	1.0	THF	1 ^b	>99	11 500	14 300	1.51	>100
4	3	400	1.0	THF	16 ^b	>99	45 800	25 900	1.50	ns
5	3	600	9.0 ^g		12	80	54 900	37 500	1.56	40
6	3	1000	9.0 ^g		12	70	80 000	40 700	1.78	58
7 ^h	3	200	1.0	THF	2	90	20 600	18 100	1.47	180
		+200	2.0	THF	6	76	34 800	32 100	1.46	25
8	7	100	2.0	CH ₂ Cl ₂	24	90	10 300	17 000	1.55	4
9	7	200	2.0	THF	10	93	21 300	18 900	1.54	19
10	7	200	9.0 ^g		1	100	22 900	24 700	1.63	>200
11	7	400	9.0 ^g		2	70	32 000	31 600	1.52	140
12	7	600	9.0 ^g		2	25	17 100	9200	1.86	75
13	7	1000	9.0 ^g		24	30	34 300	20 600	1.15	13

^a Reactions carried out at 20 °C. ^b Reaction time was not necessarily optimized. ^c Monomer conversion determined by ¹H NMR. ^d Number average molecular weight calculated from $[\text{CL}]/[\text{Al}] \times \text{conv} \times 114.4$. ^e Experimental number average molecular weight (corrected using a factor 0.56; see ref 17) and polydispersity determined by GPC in THF vs PS standards. ^f Average turnover frequency calculated over the whole reaction time. ^g Reaction conducted in bulk ϵ -caprolactone (no solvent). ^h 200 equiv of monomer added after 2 h.

Table 3. Ring-Opening Polymerization of *rac*-Lactide Promoted by $\{\text{ON}^{\text{R}}\text{NO}\}\text{Al}(\text{OiPr})$ Complexes **3 and **7**^a**

entry	compd	[LA]/[Al]	temp (°C)	time ^b (h)	conv ^c (%)	$M_{n,\text{calc}}^d$ (g/mol)	$M_{n(\text{exp})}^e$ (g/mol)	M_w/M_n^e	<i>mmm</i> ^f (%)
1 ^g	3	200	70	24	70	20 100	10 900	1.44	81
2 ^g	7	200	70	24	68	19 600	10 800	1.35	81
3	3	100	120	0.5	90	12 900	12 300	1.43	nd
4	3	200	120	0.5	92	25 600	18 200	1.91	81
5	3	400	120	0.5	87	50 100	26 400	1.73	80
6	3	400	140	0.5	87	50 100	19 300	1.39	80
7	3	1000	120	0.5	63	90 700	12 500	1.50	nd
8	7	100	130	72	70	10 100	6200	1.08	80
9	7	200	130	72	88	25 300	13 900	1.51	77
10	7	400	130	72	49	28 200	15 200	1.72	77
11	7	1000	130	72	20	28 800	13 300	1.87	nd
12	7	1,000	140	24	62	86 400	28 900	1.64	78
13	7	1000	170	0.5	50	72 000	10 500	1.27	70

^a Reactions conducted under melt conditions (no solvent, sealed lumps), unless otherwise stated. ^b Reaction time was not necessarily optimized. ^c Monomer conversion determined by ¹H NMR. ^d Number average molecular weight calculated from $[\text{LA}]/[\text{Al}] \times \text{conv} \times 144$. ^e Experimental number average molecular weight (corrected using a factor 0.58; see ref 17) and polydispersity determined by GPC in THF vs PS standards. ^f Percentage of *mmm* tetrad, as determined from the methine region of the homonuclear decoupled ¹H NMR spectrum. ^g Reaction carried out in toluene slurry at $[\text{LA}] = 2.0$ M.



However, a rather poor activity, similar for both complexes (TOF = ca. 6 h⁻¹), was observed under these reaction conditions.

Further experiments were therefore conducted in the melt (i.e., solvent-free) at 120–170 °C (entries 3–13).²⁰ Much higher activities were obtained under these conditions with **3**, leading to TOFs up to 1260 h⁻¹ at 120 °C (entry 7). The cyclohexyl-bridged complex **7** is significantly less active, with TOFs of only 2–3 h⁻¹ at 130 °C (entries 9, 10) and up to 1000 h⁻¹ at 170 °C (entry 13). Isotactic-enriched stereoblock PLAs were also formed under these conditions, with both achiral complex



Figure 11. Homonuclear decoupled ¹H NMR spectrum (500 MHz, CDCl₃, 20 °C) of the methine region of isotactic-enriched PLA (entry 2, Table 3).

3 and its chiral congener **7** leading to similar stereoselectivities. The latter do not vary much with the reaction time or the monomer-to-Al ratio, which suggests that the catalyst systems are stable over the polymerization period, at least in the temperature range 120–140 °C.²¹ Expectedly, the stereoselectivity decreases to some extent with the temperature, ranging

from 77–81% *mmm* ($P_{\text{meso}} = 0.83\text{--}0.87$) at 120–140 °C down to 70% *mmm* ($P_{\text{meso}} = 0.79$) at 170 °C. The temperature has a more pronounced effect on the M_n , inducing a noticeable decrease of these values (compare entries 5/6, 11/12/13). Only for $[\text{rac-LA}]/[\text{Al}]$ ratios < 200 are the (corrected) experimental M_n values close to the calculated ones, though still lower (entries 3, 4, 8). When the monomer loading increases ($[\text{rac-LA}]/[\text{Al}] > 200$), the difference between the experimental and the calculated M_n values increases. These observations again strongly suggest that transfer reactions take place under such conditions.

An end-group NMR study of a relatively low molecular weight PLA sample (Table 3, entry 3) indicated that, as expected, initiation of the polymerization can be envisaged to occur by the transfer of the nucleophilic isopropoxide group to the monomer with the formation of a metal alkoxide propagating species.²² Thus, in addition to the main polymer chain peaks, a P-C(O)OiPr resonance was clearly identified at δ 1.24 (2d, 6H) and 5.10 (m, 1H) ppm in the ¹H NMR spectrum (CDCl₃); additionally, a resonance for the other end-group (P-CH₂OH), obtained upon hydrolysis of the products, was observed at δ 3.66 ppm.

Conclusions

We have shown that aluminum complexes supported by fluorinated dialkoxy-diimino ligands can be prepared in high yields using straightforward procedures. Thanks to the high electron-withdrawing ability of the trifluoromethyl groups located adjacently to the alkoxides, those ligands induce the formation of discrete, mononuclear species. In most cases, a single isomer has been observed in solution and in the solid state, with geometries ranging from distorted trigonal bipyramidal to square pyramidal. Although the similarity of these fluorinated dialkoxy-diimino ligands with salen-type ligands is obvious, the replacement of rigid phenolate rings in salen ligands by sp³-hybridized alkoxide groups in the ligands of the present study results in larger flexibility, which likely accounts for the observed distorted geometries.

The isopropoxide complexes appear to be active in ROP of cyclic esters and sufficiently robust to operate ROP of lactide in the melt at high temperatures. The most interesting features revealed in this study are (i) the high dependence of polymerization activities on the nature of substituents on the ligand backbone and (ii) the significant level of isotacticity induced in the ROP of *rac*-lactide, whether a chiral or achiral ligand backbone is used. These observations open avenues for further tuning of such fluorinated alkoxide-imino ligands. Results of ongoing studies on the coordination chemistry of these original ligands with oxophilic metal centers and the application of these discrete complexes in catalysis will be reported in due course.

Experimental Section

General Procedures. All experiments were carried out under purified argon using standard Schlenk techniques or in a glovebox

(19) (a) Barakat, I.; Dubois, P.; Jerome, R.; Teyssié, P. *J. Polym. Sci., A: Polym. Chem.* **1993**, *31*, 505. (b) Ma, H.; Okuda, J. *Macromolecules* **2005**, *38*, 2665.

(20) These reactions were conducted in sealed lumps (see Experimental Section), a procedure that led to constant sublimation of lactide. We assume that part of the monomer thus “escaped” the catalyst, which accounts for the incomplete monomer conversions (i.e., entries 3–6 and 9, Table 3).

(21) The stability of complex **7** was assessed up to 120 °C by ¹H NMR (500 MHz) in C₂D₂Cl₄.

(22) (a) Yamashita, M.; Takemoto, Y.; Ihara, E.; Yasuda, H. *Macromolecules* **1996**, *29*, 1798. (b) Guillaume, S. M.; Schappacher, M.; Soum, A. *Macromolecules* **2003**, *36*, 54. (c) Sarazin, Y.; Schormann, M.; Bochmann, M. *Organometallics* **2004**, *23*, 3296.

(<1 ppm O₂, 5 ppm H₂O). Hydrocarbon solvents, diethyl ether, and tetrahydrofuran were distilled from Na/benzophenone, and toluene and pentane were distilled from Na/K alloy under nitrogen and degassed by freeze–thaw–vacuum cycles prior to use. Chlorinated solvents were distilled from calcium hydride. Deuterated solvents (>99.5% D, Eurisotop) were freshly distilled from the appropriate drying agent under argon and degassed prior to use. Pro-ligands {ON^{Et}NO}H₂ and {ON^{Cy}NO}H₂ were synthesized according to the reported procedures.¹⁰ AlMe₃, AlMe₂Cl, and Al(OiPr)₃ were purchased from Aldrich or Acros and used as received. Anhydrous hexafluoroacetone (98%) was purchased from ABCR and used as received. ϵ -Caprolactone (Acros) was dried over calcium hydride and then distilled at reduced pressure (2 mmHg, 85 °C) before use. Racemic lactide (Aldrich) was recrystallized twice from dry toluene and then sublimed under vacuum at 50 °C.

NMR spectra were recorded in Teflon-valved NMR tubes on Bruker AC-200, AC-300, and AM-500 spectrometers at 20 °C unless otherwise stated. ¹H and ¹³C NMR chemical shifts were determined using residual solvent resonances and are reported versus SiMe₄. Assignment of signals was made from 2D ¹H–¹H COSY and ¹H–¹³C HMQC and HMBC NMR experiments. ¹⁹F chemical shifts were determined by external reference to an aqueous solution of NaBF₄. All coupling constants are given in hertz. Elemental analyses (C, H, N) were performed using a Flash EA1112 CHNS Thermo Electron apparatus and are the average of two independent determinations. ESI-HRMS spectra were obtained on a high-resolution Micromass ZABSpecTOF (4 kV) MS/MS spectrometer. Size exclusion chromatography (SEC) of PCLs and PLAs was performed in THF at 20 °C using a Polymer Laboratories PL-GPC 50 Plus apparatus (PLgel 5 μ m Mixed-C 300 \times 7.5 mm, 1.0 mL/min, RI and dual angle LS (PL-LS 45/90) detectors). The number average molecular masses (M_n) and polydispersity index (M_w/M_n) of the polymers were calculated with reference to a universal calibration versus polystyrene standards. M_n values of PCLs and PLAs were corrected with a Mark–Houwink factor of 0.56¹⁷ and 0.58,¹⁹ respectively, to account for the difference in hydrodynamic volumes with polystyrene. The microstructure of PLAs was determined by homodecoupling ¹H NMR spectroscopy at 20 °C in CDCl₃ with a Bruker AC-500 spectrometer.

{^{Me}ON^{Et}NO}H₂. In a 50 mL stainless steel autoclave charged with *N,N'*-bis(2,4-dimethylpentan-3-ylidene)ethane-1,2-diamine²³ (0.56 g, 12.2 mmol) in diethyl ether (10 mL) was added hexafluoroacetone (120 mL, 5.4 mmol) at –196 °C. The reaction mixture was heated for 15 h at 50 °C. Volatiles were removed under vacuum, and the residue was recrystallized from diethyl ether to afford {^{Me}ON^{Et}NO}H₂ as a pale yellow solid (0.87 g, 67%). ¹H NMR (200 MHz, CDCl₃, 298 K): δ 1.31 (d, ³J = 7.1, 12H, CH(CH₃)₂), 1.46 (s, 12H, C(CH₃)₂), 3.12 (sept, ³J = 7.1, 2H, CH(CH₃)₂), 3.86 (s, 4H, CH₂), 11.20 (s, 2H, OH). ¹⁹F{¹H} NMR (188 MHz, CDCl₃, 298 K): δ –69.6 (s, 12F). ¹³C{¹H} NMR (50 MHz, CDCl₃, 298 K): δ 19.60 (CH₃), 23.20 (CH₃), 44.38 (CH₂), 50.80 (CH), 186.27 (C=N); resonances for the CF₃ groups were not observed, because of a too short relaxation period or a nonadapted pulse angle. ESI-HRMS: *m/z* calc for C₂₂H₃₃N₂O₂F₁₂ [M + H]⁺ 585.23504, found 585.2363 (2 ppm).

{ON^{Et}NO}AlMe (**1**). In a Schlenk flask, AlMe₃ (0.317 mL of a 2.0 M solution in heptane, 0.635 mmol) was added dropwise, at room temperature, onto a solution of pro-ligand *rac*-{ON^{Et}NO}H₂ (0.300 g, 0.635 mmol) in THF (5 mL). The reaction mixture was stirred at 50 °C for 72 h. Volatiles were then removed under vacuum, and the solid residue was washed with cold toluene (3 \times 5 mL) and dried under vacuum. Complex **1** was isolated as a white solid (0.220 g, 67%). ¹H NMR (500 MHz, CD₂Cl₂, 298 K): δ –1.01 (s, 3H, AlCH₃), 2.23 (s, 6H, NCCH₃), 2.88 (s, 4H, CH₂C(CF₃)₂), 3.57–3.77 (m, 4H, NCH₂CH₂N). ¹⁹F{¹H} NMR (182 MHz, CD₂Cl₂, 298 K): δ –78.06 (q, *J* = 10.0, 6F), –76.18 (q, *J* = 10.0,

6F). $^{13}\text{C}\{^1\text{H}\}$ NMR (75 MHz, CD_2Cl_2 , 298 K): δ -10.78 (AlCH_3), 23.44 (CCH_3), 36.77 ($\text{CH}_2\text{C}(\text{CF}_3)_2$), 47.72 ($\text{NCH}_2\text{CH}_2\text{N}$), 77.42 ($\text{CH}_2\text{C}(\text{CF}_3)_2\text{O}$), 124.60 (q, $^1J_{\text{CF}} = 282$, CF_3), 178.14 ($\text{C}=\text{N}$). Anal. Calcd for $\text{C}_{15}\text{H}_{17}\text{AlF}_{12}\text{N}_2\text{O}_2$ (512.27): C, 35.17; N, 5.47; H, 3.34. Found: C, 35.1; N, 5.5; H, 3.4.

$\{\text{ON}^{\text{Et}}\text{NO}\}\text{AlCl}$ (2**).** In a Schlenk flask, AlMe_2Cl (0.423 mL of a 1.0 M solution in hexane, 0.42 mmol) was added dropwise onto a solution of pro-ligand $\{\text{ON}^{\text{Et}}\text{NO}\}_2$ (0.200 g, 0.42 mmol) in toluene (5 mL) at room temperature. The reaction mixture was stirred at room temperature for 24 h and further heated at 60 °C for 24 h. Volatiles were then removed under vacuum, and the solid residue was washed with cold toluene (3×5 mL) and dried under vacuum. Complex **2** was isolated as a white solid (0.134 g, 60%). ^1H NMR (500 MHz, CD_2Cl_2 , 298 K): δ 2.36 (s, 6H, 2Me), 2.96 (d, $^2J = 16.0$, 2H, $\text{CHHC}(\text{CF}_3)_2$), 3.25 (d, $^2J = 16.0$, 2H, $\text{CHHC}(\text{CF}_3)_2$), 3.81 (m, 4H, $\text{NCH}_2\text{CH}_2\text{N}$). $^{19}\text{F}\{^1\text{H}\}$ NMR (182 MHz, CD_2Cl_2 , 298 K): δ -79.96 (q, $J = 10.85$, 6F), -77.95 (q, $J = 10.85$, 6F). $^{13}\text{C}\{^1\text{H}\}$ NMR (75 MHz, CD_2Cl_2 , 298 K): δ 24.33 (CH_3), 36.53 ($\text{CH}_2\text{C}(\text{CF}_3)_2$), 47.65 ($\text{NCH}_2\text{CH}_2\text{N}$), 82.11 ($\text{CH}_2\text{C}(\text{CF}_3)_2\text{O}$), 181.92 ($\text{C}=\text{N}$); quartet resonances for CF_3 groups were not observed due to their low intensity. Anal. Calcd for $\text{C}_{14}\text{H}_{14}\text{AlClF}_{12}\text{N}_2\text{O}_2$ (532.69): C, 31.57; N, 5.26; H, 2.65. Found: C, 31.6; N, 5.2; H, 2.8.

$\{\text{ON}^{\text{Et}}\text{NO}\}\text{Al}(\text{OiPr})$ (3**).** In the glovebox, a solution of pro-ligand $\{\text{ON}^{\text{Et}}\text{NO}\}_2$ (0.100 g, 0.21 mmol) in toluene (5 mL) was charged in a Schlenk flask, and $\text{Al}(\text{OiPr})_3$ (0.044 g, 0.21 mmol) was added in. The reaction mixture was vigorously stirred for 3 days at 80 °C. Volatiles were then removed under vacuum, and the residue was washed with cold hexane (2×2 mL) to afford **3** as a white powder (0.040 g, 36%). ^1H NMR (500 MHz, CD_2Cl_2 , 298 K): δ 1.01 (m, 6H, $\text{OCH}(\text{CH}_3)_2$), 2.26 (s, 6H, NCCH_3), 2.85 (d, $^2J = 15.8$, 2H, $\text{CHHC}(\text{CF}_3)_2$), 3.02 (d, $^2J = 15.8$, 2H, $\text{CHHC}(\text{CF}_3)_2$), 3.51–3.92 (m, 4H, $\text{NCH}_2\text{CH}_2\text{N}$), 4.08 (m, 1H, $\text{OCH}(\text{CH}_3)_2$). $^{19}\text{F}\{^1\text{H}\}$ NMR (182 MHz, CD_2Cl_2 , 298 K): δ -81.36 (q, $J = 10.0$, 6F), -77.68 (q, $J = 10.0$, 6F). $^{13}\text{C}\{^1\text{H}\}$ NMR (75 MHz, CD_2Cl_2 , 298 K): δ 23.07 (NCCH_3), 23.38 (NCCH_3), 27.16 ($\text{OCH}(\text{CH}_3)_2$), 36.40 ($\text{CH}_2\text{C}(\text{CF}_3)_2$), 37.02 ($\text{CH}_2\text{C}(\text{CF}_3)_2$), 47.72 ($\text{NCH}_2\text{CH}_2\text{N}$), 49.80 ($\text{NCH}_2\text{CH}_2\text{N}$), 62.72 ($\text{OCH}(\text{CH}_3)_2$), 77.34 ($\text{CH}_2\text{C}(\text{CF}_3)_2\text{O}$), 124.00 (q, $^1J_{\text{CF}} = 222$, CF_3), 178.55 ($\text{C}=\text{N}$). Anal. Calcd for $\text{C}_{17}\text{H}_{21}\text{AlF}_{12}\text{N}_2\text{O}_3$ (556.32): C, 36.70; N, 5.04; H, 3.80. Found: C, 36.6; N, 5.1; H, 3.8.

$\text{rac-}\{\text{ON}^{\text{Cy}}\text{NO}\}\text{AlMe}$ (rac-5**).** In a Schlenk flask, a solution of pro-ligand $\text{rac-}\{\text{ON}^{\text{Cy}}\text{NO}\}_2$ (0.200 g, 0.38 mmol) in THF (10 mL), precooled at -30 °C, was added dropwise onto a solution of AlMe_3 (0.19 mL of a 2.0 M solution in heptane, 0.38 mmol) in THF (5 mL), precooled at -30 °C. The reaction mixture was stirred at room temperature for 24 h and further heated at 50 °C for 24 h. Volatiles were then removed under vacuum, and the solid residue was washed with cold toluene (3×5 mL) and dried under vacuum. Complex **rac-5** was isolated as a white solid (0.135 g, 63%). ^1H NMR (500 MHz, CD_2Cl_2 , 298 K): δ -0.89 (s, 3H, AlCH_3), 1.39–1.62 (m, 4H, $\gamma\text{-CH}_2\text{CH}_2$ cyclohexyl), 1.79–1.84 (m, 2H, $\beta\text{-CH}_2$ cyclohexyl), 1.99–2.09 (m, 2H, $\beta\text{-CH}_2$ cyclohexyl), 2.14 (s, 3H, CCH_3), 2.27 (s, 3H, CCH_3), 2.79–3.10 (m, 4H, $\text{CH}_2\text{-C}(\text{CF}_3)_2$), 3.19 (t, $J = 10.9$, 1H, $\text{CH-N}=\text{C}$), 4.20 (t, $J = 10.9$, 1H, $\text{CH-N}=\text{C}$). $^{19}\text{F}\{^1\text{H}\}$ NMR (182 MHz, CD_2Cl_2 , 298 K): δ -80.06 (q, $J = 10.3$, 3F), -79.61 (q, $J = 10.3$, 3F), -78.43 (q, $J = 8.7$, 3F), -77.57 (q, $J = 8.7$, 3F). $^{13}\text{C}\{^1\text{H}\}$ NMR (75 MHz, CD_2Cl_2 , 298 K): δ -8.68 (AlCH_3), 23.13 (CCH_3), 24.17 ($\text{CH}_2\text{CH}_2\text{CHN}$ cyclohexyl), 24.47 (CCH_3), 25.77 ($\text{CH}_2\text{CH}_2\text{CHN}$ cyclohexyl), 31.53 (CH_2CHN cyclohexyl), 31.72 (CH_2CHN cyclohexyl), 36.36 ($\text{CH}_2\text{C}(\text{CF}_3)_2$), 38.46 ($\text{CH}_2\text{C}(\text{CF}_3)_2$), 64.26 (CHNC cyclohexyl), 65.26 (CHNC cyclohexyl), 77.70 ($\text{CH}_2\text{C}(\text{CF}_3)_2\text{O}$), 77.76 ($\text{CH}_2\text{C}(\text{CF}_3)_2\text{O}$), 124.16 (q, $^1J_{\text{CF}} = 290$ Hz, CF_3), 171.58 ($\text{C}=\text{N}$), 179.02 ($\text{C}=\text{N}$). Anal. Calcd for $\text{C}_{19}\text{H}_{23}\text{AlF}_{12}\text{N}_2\text{O}_2$ (566.37): C, 40.29; N, 4.95; H, 4.09. Found: C, 40.4; N, 4.8; H, 4.2.

$\text{rac-}\{\text{ON}^{\text{Cy}}\text{NO}\}\text{AlCl}$ (rac-6**).** This complex was prepared following a similar procedure to that described above for **rac-5**, starting from a solution of $\text{rac-}\{\text{ON}^{\text{Cy}}\text{NO}\}_2$ (0.100 g, 0.19 mmol) in toluene (10 mL) and AlMe_2Cl (0.19 mL of a 1.0 M solution in hexane (0.19 mmol)). Reaction for 48 h at 50 °C and workup afforded **rac-6** as a white powder (0.090 g, 81%). ^1H NMR (500 MHz, CD_2Cl_2 , 298 K): δ 1.51–2.19 (m, 8H, β - and $\gamma\text{-CH}_2$ cyclohexyl), 2.29 (s, 3H, CH_3), 2.39 (s, 3H, CH_3), 2.88 (m, 2H, $\text{CH}_2\text{C}(\text{CF}_3)_2$), 3.09 (m, 2H, $\text{CH}_2\text{C}(\text{CF}_3)_2$), 3.31 (t, $J = 3.1$, 1H, CH-NC), 4.45 (t, $J = 3.1$, 1H, CH-NC). $^{19}\text{F}\{^1\text{H}\}$ NMR (182 MHz, CD_2Cl_2 , 298 K): δ -80.09 (q, $J = 10.35$, 3F), -79.63 (q, $J = 10.35$, 3F), -78.40 (q, $J = 10.35$, 3F), -77.55 (q, $J = 10.35$, 3F). $^{13}\text{C}\{^1\text{H}\}$ NMR (75 MHz, CD_2Cl_2 , 298 K): δ 24.04 (NCCH_3), 24.80 (NCCH_3), 25.55 ($\text{CH}_2\text{CH}_2\text{CHN}$ cyclohexyl), 31.28 (CH_2CHN cyclohexyl), 31.65 (CH_2CHN cyclohexyl), 36.09 ($\text{CH}_2\text{C}(\text{CF}_3)_2$), 38.46 ($\text{CH}_2\text{C}(\text{CF}_3)_2$), 63.96 (CH-NC cyclohexyl), 65.81 (CH-NC cyclohexyl), 76.86 ($\text{CH}_2\text{C}(\text{CF}_3)_2\text{O}$), 77.24 ($\text{CH}_2\text{C}(\text{CF}_3)_2\text{O}$), 173.56 ($\text{C}=\text{N}$), 183.32 ($\text{C}=\text{N}$); quartet resonances for CF_3 groups were not observed due to their low intensity. Anal. Calcd for $\text{C}_{18}\text{H}_{20}\text{AlClF}_{12}\text{N}_2\text{O}_2$ (586.78): C, 36.84; N, 4.77; H, 3.44. Found: C, 37.0; N, 4.8; H, 3.6.

$(1R,2R)\text{-}\{\text{ON}^{\text{Cy}}\text{NO}\}\text{AlCl}$ (6**).** This complex was prepared as described above for **rac-6**, starting from a solution of $(1R,2R)\text{-}\{\text{ON}^{\text{Cy}}\text{NO}\}_2$ (0.100 g, 0.19 mmol) in toluene (10 mL) and AlMe_2Cl (0.19 mL of a 1.0 M solution in hexane, 0.19 mmol). Reaction for 48 h at 50 °C and workup afforded **6** as a white powder (0.078 g, 70%). ^1H , ^{19}F , and ^{13}C NMR data were identical to those of **rac-6**. $[\alpha]_D^{20}$ (CH_2Cl_2 , c 0.01) = -100.

$(1R,2R)\text{-}\{\text{ON}^{\text{Cy}}\text{NO}\}\text{Al}(\text{OiPr})$ (7**).** In the glovebox, a solution of pro-ligand $(1R,2R)\text{-}\{\text{ON}^{\text{Cy}}\text{NO}\}_2$ (0.100 g, 0.19 mmol) in toluene (5 mL) was charged in a Schlenk flask, and $\text{Al}(\text{OiPr})_3$ (0.039 g, 0.19 mmol) was added in. The reaction mixture was vigorously stirred for 3 days at 80 °C. Volatiles were then removed under vacuum, and the residue was washed with cold hexane (2×2 mL) to afford **7** as a white powder (0.065 g, 56%). ^1H NMR (500 MHz, CD_2Cl_2 , 298 K): δ 1.03 (m, 6H, $\text{OCH}(\text{CH}_3)_2$), 1.38–2.07 (m, 8H, β - and $\gamma\text{-CH}_2$ cyclohexyl), 2.18 (s, 3H, NCCH_3), 2.27 (s, 3H, NCCH_3), 2.48–3.07 (m, 4H, $\text{CH}_2\text{C}(\text{CF}_3)_2$), 3.17 (t, $J = 3.1$, 1H, CHNC), 4.12 (m, 1H, $\text{OCH}(\text{CH}_3)_2$), 4.46 (t, $J = 3.1$, 1H, CHNC). $^{19}\text{F}\{^1\text{H}\}$ NMR (182 MHz, CD_2Cl_2 , 298 K): δ -80.35 (q, $J = 10.35$, 3F), -79.90 (q, $J = 10.35$, 3F), -78.30 (q, $J = 10.35$, 3F), -77.55 (q, $J = 10.35$, 3F). $^{13}\text{C}\{^1\text{H}\}$ NMR (75 MHz, CD_2Cl_2 , 298 K): δ 23.40 (CCH_3), 24.22 (CCH_3), 24.51 ($\text{CH}_2\text{CH}_2\text{CHN}$ cyclohexyl), 25.80 ($\text{CH}_2\text{CH}_2\text{CHN}$ cyclohexyl), 27.24 ($\text{OCH}(\text{CH}_3)_2$), 31.29 (CH_2CHN cyclohexyl), 31.66 (CH_2CHN cyclohexyl), 36.33 ($\text{CH}_2\text{C}(\text{CF}_3)_2$), 38.59 ($\text{CH}_2\text{C}(\text{CF}_3)_2$), 62.80 ($\text{OCH}(\text{CH}_3)_2$), 64.11 (CHNC cyclohexyl), 65.74 (CHNC cyclohexyl), 77.44 ($\text{CH}_2\text{C}(\text{CF}_3)_2\text{O}$), 77.54 ($\text{CH}_2\text{C}(\text{CF}_3)_2\text{O}$), 124.11 (q, $^1J_{\text{CF}} = 64$ Hz, CF_3), 171.14 ($\text{C}=\text{N}$), 181.75 ($\text{C}=\text{N}$). $[\alpha]_D^{20}$ (CH_2Cl_2 , c 0.01) = -200. Anal. Calcd for $\text{C}_{21}\text{H}_{27}\text{AlF}_{12}\text{N}_2\text{O}_3$ (610.43): C, 41.32; N, 4.59; H, 4.46. Found: C, 41.2; N, 4.7; H, 4.5.

$\{\text{MeON}^{\text{Et}}\text{NO}\}\text{AlMe}$ (8**).** This complex was prepared as described for **1**, starting from $\{\text{MeON}^{\text{Et}}\text{NO}\}_2$ (0.100 g, 0.17 mmol) and AlMe_3 (0.17 mmol) in THF (15 mL) and reacting for 48 h at 50 °C. Workup afforded **8** as a white solid (0.073 g, 68%). Crystals of **8** suitable for X-ray diffraction were prepared by prolonged crystallization from a toluene solution at -30 °C. At 248 K, two sets of sharp signals were observed in the ^1H and $^{13}\text{C}\{^1\text{H}\}$ NMR (HMBC/HMQC) NMR, consistent with the existence of two isomers of **8** (**8a** and **8b**) in a 2:1 molar ratio and in slow exchange on the NMR time scale. ^1H NMR (500 MHz, CD_2Cl_2 , 248 K): δ -0.96 (s, 3H, AlCH_3 , **a**), -0.92 (s, 3H, AlCH_3 , **b**), 1.30 (m, 12H, $\text{CH}(\text{CH}_3)_2$, **a** and **b**), 1.38 (br s, 6H, $\text{C}(\text{CH}_3)_2$, **a** and **b**), 1.55 (br s, 6H, $\text{C}(\text{CH}_3)_2$, **a** and **b**), 3.37 (sept, $^3J = 5.0$, 2H, $\text{CH}(\text{CH}_3)_2$, **a**), 3.44 (sept, $^3J = 5.0$, 2H, $\text{CH}(\text{CH}_3)_2$, **b**), 3.57 (m, 1H, $\text{CHH-C}=\text{N}$, **a**), 3.90 (m, 2H, $\text{CHH-C}=\text{N}$, **a**), 4.07 (m, 1H, $\text{CHH-C}=\text{N}$, **a**), 3.70 (m, 2H, $\text{CH}_2\text{-C}=\text{N}$, **b**), 3.78 (m, 2H, $\text{CH}_2\text{-C}=\text{N}$, **b**). $^{19}\text{F}\{^1\text{H}\}$

NMR (188 MHz, CD₂Cl₂, 298 K): δ -70.97 (2 s, ca. 12F, **a** and **b**), -69.24 (br s, ca. 6F, **a**). ¹³C{¹H} NMR (HMBC/HMQC) (75 MHz, CD₂Cl₂, 248 K): δ -4.93 (AlCH₃, **b**), -4.36 (AlCH₃, **a**), 18.91, 19.17, 19.88, 19.80, 19.73 (CH(CH₃)₂, **a** and **b**), 20.68, 21.31, 21.77, 23.82, 27.68 (C(CH₃)₂, **a** and **b**), 30.95 (CH(CH₃)₂, **a**), 31.58 (CH(CH₃)₂, **b**), 46.41, 46.73, 47.92, 46.89 (C(CH₃)₂, **a** and **b**), 48.66 (CH₂, **b**), 48.14 (CH₂, **a**), 49.93 (CH₂, **a**), 194.81 (C=N, **a**), 197.62 (C=N, **b**). Anal. Calcd for C₂₃H₃₃AlF₁₂N₂O₂ (624.48): C, 44.24; N, 4.49; H, 5.33. Found: C, 44.2; N, 4.6; H, 5.2.

{^{Me}ON^{Et}NO}AlCl (**9**). This complex was prepared as described for **2**, starting from {^{Me}ON^{Et}NO}H₂ (0.100 g, 0.17 mmol) and AlMe₂Cl (0.17 mL of a 1.0 M solution, 0.17 mmol) in toluene (15 mL) and reacting for 48 h at 50 °C. Workup afforded **9** as a white solid (0.068 g, 62%). At 248 K, two sets of sharp signals were observed in the ¹H and ¹³C{¹H} NMR (HMBC/HMQC) NMR, consistent with the existence of two isomers of **9** (**9a** and **9b**) in 1.2:1 molar ratio. ¹H NMR (500 MHz, CD₂Cl₂, 248 K): δ 1.36 (m, 12H, CH(CH₃)₂, **a** and **b**), 1.56 (m, 12H, C(CH₃)₂, **a** and **b**), 3.40 (sept, 1H, ³J = 7.0, CH(CH₃)₂, **b**), 3.53 (sept, 1H, ³J = 7.0, CH(CH₃)₂, **b**), 3.43 (sept, 2H, ³J = 7.0, CH(CH₃)₂, **a**), 3.69 (m, 2H, CHH-C=N, **a**), 3.98 (m, 2H, CHH-C=N, **a**), 3.69 (m, 1H, CHH-C=N, **b**), 3.77 (m, 1H, CHH-C=N, **b**), 4.20 (m, 1H, CHH-C=N, **b**), 4.32 (m, 1H, CHH-C=N, **b**). ¹⁹F{¹H} NMR (188 MHz, CD₂Cl₂, 298 K): δ -70.65 (br s, 12F), -68.91 (br s, 12F) (**a** and **b**). ¹³C NMR (HMBC/HMQC) (75 MHz, CD₂Cl₂, 248 K): δ 18.41, 18.58, 19.03, 19.16, 19.39 (CH(CH₃)₂, **a** and **b**), 20.71, 21.04, 22.11, 22.87, 23.69 (C(CH₃)₂, **a** and **b**), 30.97, 32.00, 32.03 (CH(CH₃)₂, **a** and **b**), 46.74, 47.51 (C(CH₃)₂, **a** and **b**), 50.01 (CH₂, **a**), 48.17, 48.78 (CH₂, **b**), 192.62 (C=N, **b**), 198.39 (C=N, **a**), 201.45 (C=N, **b**). Anal. Calcd for C₂₂H₃₀AlClF₁₂N₂O₂ (644.91): C, 40.97; N, 4.34; H, 4.69. Found: C, 41.0; N, 4.4; H, 4.7.

Crystal Structure Determination of {ON^{Cy}NO}H₂, {^{Me}ON^{Et}NO}H₂, **4, **5**, **7**, **8**, and **9**.** Suitable crystals for X-ray diffraction analysis of {ON^{Cy}NO}H₂, {^{Me}ON^{Et}NO}H₂, **5**, **7**, **8**, and **9** were obtained by recrystallization of purified products. Crystals of **4** were obtained upon attempting recrystallization of complex **3**. Diffraction data were collected at 100 K using a Bruker APEX CCD diffractometer with graphite-monochromatized Mo K α radiation (λ = 0.71073 Å). A combination of ω and ϕ scans was carried out to obtain at least a unique data set. The crystal structures were solved by means of the Patterson method; the remaining atoms were located from difference Fourier synthesis followed by full matrix least-squares refinement based on F^2 (programs SHELXS-97 and SHELXL-97).²⁴ Many hydrogen atoms could be found from the Fourier difference analysis. Carbon- and oxygen-bound hydrogen atoms were placed at calculated positions and forced to ride on the attached atom. The hydrogen atom contributions were calculated but not refined. All non-hydrogen atoms were refined with anisotropic displacement parameters. The locations of the largest peaks in the final difference Fourier map calculation as well as the magnitude of the residual electron densities were of no chemical significance. In {ON^{Cy}NO}H₂ and **4**, the methyl groups were found

to be disordered and accordingly modeled. Similarly, in **8**, two trifluoromethyl groups were found to be disordered and accordingly modeled. The PLATON checkcif procedure for **7** found a pseudosymmetry center and suggested $P\bar{1}$ as an alternative space group. Although all non-hydrogen atoms could be refined anisotropically within this group, the R (0.1100) and R_{int} (0.1386) factors were significantly larger than processing the data in the $P1$ space group (0.0700 and 0.0846, respectively), thus corroborating the validity of the later space group (cyclohexyl groups were also found to be planar upon processing in the $P\bar{1}$ space group). Crystallographic data (excluding structure factors) for the structures in this paper have been deposited with the Cambridge Crystallographic Data Centre as supplementary publication nos. 692408–692414 for {ON^{Cy}NO}H₂, {^{Me}ON^{Et}NO}H₂, **4**, **5**, **7**, **8**, and **9**. Copies of the data can be obtained, free of charge, on application to CCDC, 12 Union Road, Cambridge CB2 1EZ, UK (fax: +44-(0)1223-336033 or e-mail: deposit@ccdc.cam.ac.uk).

Typical Procedure for ϵ -Caprolactone Polymerization (Table 2, entries 1–13). A Schlenk flask was charged with a solution of **3** in CH₂Cl₂ or THF. To this solution was rapidly added under stirring a solution of ϵ -caprolactone in the appropriate ratio in CH₂Cl₂ or THF. The reaction mixture was stirred at the desired temperature for the desired reaction time. After an aliquot of the crude solution was removed for analytical purposes, the reaction was quenched with acidic methanol (0.5 mL), and the polymer was precipitated with excess methanol. The polymer was then dried *in vacuo* to constant weight. Polymerization runs of *rac*-lactide in toluene slurry (Table 3, entries 1 and 2) were conducted following a similar procedure.

Typical Procedure for *rac*-Lactide Polymerization in the Melt (Table 3, entries 3–13). In the glovebox, a ca. 10 mL glass lump was charged with **3** (10.0 mg, 0.018 mmol), *rac*-LA (519 mg, 3.59 mmol), and a magnetic stir bar. The lump was sealed under vacuum and immersed in an oil bath at 130 °C with magnetic stirring. After 72 h, the lump was taken off, cooled to room temperature, and opened in air. An aliquot was analyzed by ¹H NMR spectrometry for determining the conversion. About 0.5 mL of acidic methanol (1.2 M HCl solution in CH₃OH) was added in the lump and the polymer was precipitated with excess methanol (ca. 3 mL). Then, the supernatant solution was removed with a pipet and the polymer was dried under vacuum to constant weight.

Acknowledgment. This work was financially supported in part by Agence Nationale de la Recherche (grant ANR-06-BLAN-0213). M.B. thanks the Ministère de l'Enseignement Supérieur et de la Recherche for a Ph.D. fellowship. J.F.C. gratefully thanks the Institut Universitaire de France for a Junior IUF fellowship (2005–2009).

Supporting Information Available: Crystallographic data as cif files for pro-ligands {ON^{Cy}NO}H₂ and {^{Me}ON^{Et}NO}H₂ and complexes **4**, **5**, **7**, **8**, and **9**. This material is available free of charge via the Internet at <http://pubs.acs.org>.

OM800651Z

(24) (a) Sheldrick, G. M. *SHELXS-97*, Program for the Determination of Crystal Structures; University of Goettingen (Germany), 1997. (b) Sheldrick, G. M. *SHELXL-97*, Program for the Refinement of Crystal Structures; University of Goettingen (Germany), 1997.